Microbiological Research 177 (2015) 15–21

Contents lists available at ScienceDirect

Microbiological Research

journal homepage: www.elsevier.com/locate/micres

# The ActP acetate transporter acts prior to the PitA phosphate carrier in tellurite uptake by *Escherichia coli*

Alex Elías[a,b,1], Waldo Díaz-Vásquez[a,b,1], María José Abarca-Lagunas[a], Thomas G. Chasteen[c], Felipe Arenas[a], Claudio C. Vásquez[a,*]

[a] Departamento de Biología, Facultad de Química y Biología, Universidad de Santiago de Chile, Santiago, Chile
[b] Facultad de Ciencias de la Salud, Universidad San Sebastián, Santiago, Chile
[c] Department of Chemistry and Texas Research Institute for Environmental Studies, Sam Houston State University, Huntsville, TX, USA

ARTICLE INFO

*Article history:*
Received 6 February 2015
Received in revised form 20 April 2015
Accepted 25 April 2015
Available online 8 May 2015

*Keywords:*
ActP
Tellurite uptake
*Escherichia coli*

ABSTRACT

The tellurium oxyanion tellurite is harmful for most microorganisms. Since its toxicity occurs chiefly once the toxicant reaches the intracellular compartment, unveiling the toxicant uptake process is crucial for understanding the whole phenomenon of tellurium toxicity. While the PitA phosphate transporter is thought to be one of the main paths responsible for toxicant entry into *Escherichia coli*, genetic and physiological evidence have identified the ActP acetate carrier as the main tellurite importer in *Rhodobacter capsulatus*. In this work, new background on the role of these transporters in tellurite uptake by *E. coli* is presented. It was found that, similar to what occurs in *R. capsulatus*, ActP is able to mediate toxicant entry to this bacterium. Lower reactive oxygen species levels were observed in *E. coli* lacking the actP gene.

Antioxidant enzyme catalase and fumarase C activity was almost unchanged after short exposure of *E. coli* Δ*actP* to sublethal tellurite concentrations, suggesting a low antioxidant response. In this strain, tellurite uptake decreased significantly during the first 5 min of exposure and inductively coupled plasma optical emission spectroscopy assays using an *actP*-overexpressing strain confirmed that this carrier mediates toxicant uptake. Relative gene expression experiments by qPCR showed that *actP* expression is enhanced at short times of tellurite exposure, while *pitA* and *pitB* genes are induced later. Summarizing, the results show that ActP is involved in tellurite entry to *E. coli* and that its participation occurs mainly at early stages of toxicant exposure.



## 1. Introduction

Tellurium (Te), a rather scarce element in the Earth's crust, has no known biological role to date. Occasionally Te is found as elemental tellurium ($Te^0$), but it most commonly forms alloys with metals like gold and silver. On the other hand, tellurium oxyanions tellurite ($TeO_3^{2-}$) and tellurate ($TeO_4^{2-}$) are well known for their toxicity (Taylor, 1999; Chasteen et al., 2009). The more soluble of these two, tellurite, is extremely noxious for microorganisms and has been used as selective agent in microbiology for decades (Fleming, 1932). In fact, regarding *Escherichia coli* minimal inhibitory concentrations, tellurite is by far more toxic than other metal(loid)s including mercury and silver (Nies, 1999).

However, the molecular foundation underlying tellurite toxicity is not completely clarified. At least part of it seems to be a consequence of its strong oxidant properties, which, to the end, results in the formation of reactive oxygen species (ROS) that damage cell macromolecules (Borsetti et al., 2005; Pérez et al., 2007; Calderón et al., 2009; Castro et al., 2008; Pradenas et al., 2013). On the other hand, reduced thiols like glutathione are among the main intracellular tellurite targets (Turner et al., 1999). Also, it has been suggested that upon tellurite exposure, Te can replace S and/or Se, thus inactivating defined proteins (Taylor, 1999; Cunha et al., 2009).

In spite of this, there are naturally-occurring tellurite-resistant bacteria that often reduce tellurite to elemental tellurium which accumulates as black intracellular deposits (Chiong et al., 1988; Moscoso et al. 1998), a process which could represent a first line of resistance/defense against the toxicant (Taylor, 1999). Along the same line, other bacteria detoxify tellurite by producing alkylated tellurium derivatives such as dimethyl tellurium and dimethyl ditelluride (Chasteen and Bentley, 2003; Araya et al., 2004; Chasteen et al., 2009).

* Corresponding author. Tel.: +56 2 2718 1117.
*E-mail address:* claudio.vasquez@usach.cl (C.C. Vásquez).
[1] These authors contributed equally to this work.

http://dx.doi.org/10.1016/j.micres.2015.04.010
0944-5013/

Currently, bacterial tellurite resistance is considered a multifactor response that involves, directly or indirectly, substrates and/or products of a number of metabolic pathways (Acuña et al., 2009; Castro et al., 2008, 2009; Valdivia-González et al., 2012). Given that tellurite exerts toxic effects only once it is inside the cell, it is mandatory to unveil the mechanism by which tellurite is transported from the extracellular space. In this context, while *E. coli* mutants lacking phosphate transport systems exhibited high tellurite tolerance (Tomás and Kay, 1986), alterations of the Pst phosphate transport system or the ChoQ protein resulted in a similar phenotype in *Lactococcus lactis* (Turner et al., 2007). Additional evidence showed that tellurite uptake is a pH-dependent process in *Rhodobacter capsulatus* (Borsetti et al., 2003). Later, the same group showed the active participation of the ActP monocarboxylate transporter in tellurite uptake (Borghese et al., 2008; Borghese and Zannoni, 2010). Finally, our group demonstrated that, at least in *E. coli*, tellurite transport is mediated mainly by the PitA phosphate transporter (Elías et al., 2012). In this work, the eventual participation of ActP was assessed in *E. coli.*

## 2. Materials and methods

### 2.1. Bacterial strains and growth conditions

*E. coli* BW25113 (*lacI*$^q$ *rrnB*$_{T14}$Δ*lacZ*$_{WJ16}$ *hsdR*514 Δ*araBAD*$_{AH33}$Δ*rhaBAD*$_{LD78}$, (parental) and the isogenic, kanamycin-resistant, derivatives JW4028 (Δ*actP*), JW3578 (Δ*lacY*), JW2942 (Δ*glcA*), JW3898 (Δ*glpF*), JW3460 (Δ*pitA*) and JW2955 (Δ*pitB*) were from the KEIO collection of the National Institute of Genetics, Japan (Baba et al., 2006). *E. coli* AG1 (*endA*1 *recA*1 *gyrA*96 *thi*-1 *relA*1 *glnV*44 *hsdR*17 [$r_K^- m_K^+$], parental) and the ASKA derivatives that over-express cloned *actP* or *pitA* genes in the presence of 1 mM IPTG (Kitagawa et al., 2005) were obtained from the same source. Cell growth either in LB or M9 minimal medium supplemented with 0.2% glucose (Sambrook and Russell, 2001) was routinely started by inoculating pre-warmed fresh media with 1:100 (M9) or 1:1000 (LB) dilutions of overnight cultures. When required, kanamycin (10 μg ml$^{-1}$) or chloramphenicol (30 μg ml$^{-1}$) was added to the medium. Unless otherwise stated tellurite concentration was 20 μM. Growth was monitored at 600 nm in a TECAN INFINITE 200 PRO microplate reader.

### 2.2. Determination of growth inhibition areas and minimal inhibitory concentration

Bacteria were evenly spread in M9 minimal medium (containing 0.2% glucose) or LB agar (2%) plates amended with the appropriate antibiotic(s) when needed. Growth inhibition zones (GIZs) in the presence of defined metal ions were determined as described earlier (Fuentes et al., 2007).

Tellurite MIC was assessed in M9 minimal medium supplemented with 0.2% glucose. Aliquots (5 μl) of overnight cultures were mixed with 200 μl of medium deposited in 96-well microplates that contained increasing $TeO_3^{-2}$concentrations. Serial dilutions were performed starting with a sterile 400 μM solution. After overnight incubation at 37 °C, the minimal toxicant concentration inhibiting bacterial growth was determined.

### 2.3. Cell viability

Saturated cultures of *E. coli* BW25113 or mutant derivatives were diluted (1:100) with fresh M9-glucose medium and incubated at 37 °C with constant shaking to $OD_{600} \sim 0.05$. Cultures were again diluted 1:100 with the same medium (pre-warmed at 37 °C) and growth was continued to $OD_{600} \sim 0.15$. Then, $TeO_3^{-2}$ was added (controls received sterile water) and at different time intervals aliquots were taken, diluted $10^6$ fold, and plated in M9-glucose agar. After incubating overnight at 37 °C, the number of colony forming units (CFU) was determined.

### 2.4. Assessing ROS production

Total intracellular ROS and superoxide were determined using dihydrodichlorofluorescein diacetate ($H_2$DCFDA, $\lambda_{ex}$ 490 nm–$\lambda_{em}$ 522 nm) and dihydroethidine (DHE, $\lambda_{ex}$ 520 nm, $\lambda_{em}$ 610 nm), respectively. After tellurite exposure, cells were centrifuged at 8000 × *g* for 3 min at 4 °C and washed with 50 mM Tris–HCl buffer, pH 7.4. The pellet was suspended in 1 ml of the same buffer and shaken with the probes (20 μM) for 30 ($H_2$DCFDA) or 15 (DHE) min at 37 °C in the dark. Then, optical density and fluorescence were determined in the TECAN apparatus.

### 2.5. Preparation of crude protein extracts

Cultures were centrifuged at 10,000 × *g* for 10 min at 4 °C, washed 2X with 2 ml of 50 mM potassium phosphate buffer, pH 7.4 (buffer A), and suspended in 1 ml of the same buffer. After adding the protease inhibitor PMSF (1 mM, final concentration) cells were disrupted by sonication and the cell debris was discarded by centrifuging as above. The supernatant was considered the crude extract, and protein concentration was determined as described previously (Bradford, 1976).

### 2.6. Enzyme activity

#### 2.6.1. Catalase

The enzyme was assayed for 2 min by monitoring $H_2O_2$ decomposition at 240 nm. The reaction mix (1 ml) contained 50 mM potassium phosphate buffer, pH 7.0 and 19.4 mM $H_2O_2$. The reaction was started with the crude extract (45 μg protein) as described elsewhere (Chen and Schellhorn, 2003).

#### 2.6.2. Fumarase C

The enzyme activity was assessed by measuring the formation of fumarate from L-malate for 2 min at 250 nm using the crude extract (15 μg protein). A molar extinction coefficient of 1.62 mM$^{-1}$ cm$^{-1}$ was used (Liochev and Fridovich, 1992).

### 2.7. Extracellular tellurite concentration

*E. coli* grown to $OD_{600} \sim 0.15$ was treated with tellurite (20 μM) and aliquots were taken at various time intervals to determine remaining tellurite in the supernatant as described previously (Molina et al., 2010).

### 2.8. Te quantification by inductively coupled plasma optical emission spectroscopy (ICP-OES)

Cells previously exposed to tellurite (1/2 MIC) were washed, suspended in 1 ml of buffer A and sonicated gently. Samples were diluted 10-fold with 10% $HNO_3$ and the whole volume was used for Te determination using a Spectro CIROS Vision ICP-OES apparatus as previously described (Díaz-Vásquez et al., 2014a). A calibration curve was constructed with commercially-available tellurium standards (Sigma).

### 2.9. Relative gene expression

Total RNA was prepared from cells grown in LB medium and exposed to tellurite (1/2 MIC) for 5, 10 and 15 min using the Favorprep tissue total RNA purification mini kit (Favorgene) and quantified using the Quant-it Ribogreen Kit (Invitrogen). qRT-PCR

was carried out using a Light Cycler apparatus with the RNA Master SYBR Green Kit (Roche Applied Science). One hundred ng of purified RNA were used as template. *rpoD* and *gapA* were used as the housekeeping genes. Transcript levels were calculated using the ΔΔCt method (Livak and Schmittgen, 2001). Specific primers to amplify the genes being studied are shown in Table S1.

### 2.10. Data analysis

Data analysis was carried out using the GraphPad Prism® 5 software. Unless otherwise stated the results were expressed as the average of at least 3 different trials ± SE using analysis of variance (ANOVA), $p < 0.05$(*), $p < 0.001$(**), $p < 0.001$(***).

## 3. Results

Previous results from Borghese et al. (2008) indicated that tellurite uptake by *R. capsulatus* was inhibited by carboxyl group-containing compounds such as pyruvate, lactate and acetate. Later, the same group identified the ActP acetate transporter as responsible for toxicant entrance to this bacterium (Borghese and Zannoni, 2010). On the other hand, results from our group indicated that tellurite entry to *E. coli* occurred mainly through the PitA phosphate transporter (Elías et al., 2012). These apparently contrasting observations were interpreted as valid because they came from different microorganisms and prompted us to evaluate more in depth the participation of ActP in tellurite uptake by *E. coli*.

### 3.1. Studies of tellurite transport in E. coli

As mentioned before and because monocarboxylate transporters have been involved in tellurite entry in *R. capsulatus* (Borghese et al., 2008; Borghese and Zannoni, 2010), a number of *E. coli* mutants lacking acetate (ActP), lactate (LacY) or glycolate (GlcA) transporters were assessed for toxicant uptake. Moreover, since the glycerol facilitator channel GlpF convey antimonite and arsenite (Meng et al., 2004; Sanders et al., 1997) – molecules that share structural similarity with tellurite – this channel was also analyzed for tellurite entry. The *E. coli* Δ*pitA* strain was included as control.

**Table 1**
Tellurite minimal inhibitory concentration (μM), growth inhibition zones ($cm^2$) and visual inspection determination for *E. coli* exposed for the indicated times to tellurite; +, ++ and +++, relative intensity of the black color of tellurite-exposed cultures; –, no color.

| *E. coli* strain | GIZ | MIC | Cells/culture color | | |
|---|---|---|---|---|---|
| | | | 5 min | 15 min | 30 min |
| BW25113 | 7.0 ± 1.0 | 50 | + | ++ | +++ |
| Δ*actP* | 6.3 ± 0.6 | 120 | – | + | ++ |
| Δ*glpF* | 6.6 ± 0.5 | 80 | + | ++ | ++ |
| Δ*glcA* | 6.9 ± 0.5 | 50 | + | ++ | +++ |
| Δ*lacY* | 7.1 ± 0.7 | 50 | + | ++ | +++ |
| Δ*pitA* | 4.8 ± 0.7 | 200 | + | + | + |

Growth inhibition zones, minimal inhibitory concentrations, cell viability assays and cell color after tellurite treatment were assessed in exposed and unexposed cells (Table 1). It was observed that mainly Δ*actP* and, to a lesser extent, the Δ*glpF* strain exhibited augmented tellurite resistance regarding the parental control. However, in nearly all the subsequent experiments, an almost identical behavior was observed when Δ*glpF* cells were compared to the respective controls. This could be a consequence of the *glpF* down-regulation in the presence of tellurite (Molina-Quiroz et al., 2014) and it was not analyzed further. On the other hand, cells lacking *lacY* or *glcA* did not show significant differences when compared to the control strain (Table 1). Interestingly, even when a decrease of cell viability was observed at short incubations with sub lethal toxicant concentrations, the viability of Δ*actP* cells was higher afterwards than that of the wild type control and followed the same trend as the Δ*pitA* strain (Fig. 1). However, all strains tested showed a lag phase that lasted almost 10 h before going into exponential growth. It is interesting to note that the Δ*actP* strain (carries a functional *pitA* gene) takes even more time to make growth progress (Fig. S1).

To assess if the studied mutations affect the toxicity of oxidative stressors other than tellurite, growth inhibition zones were

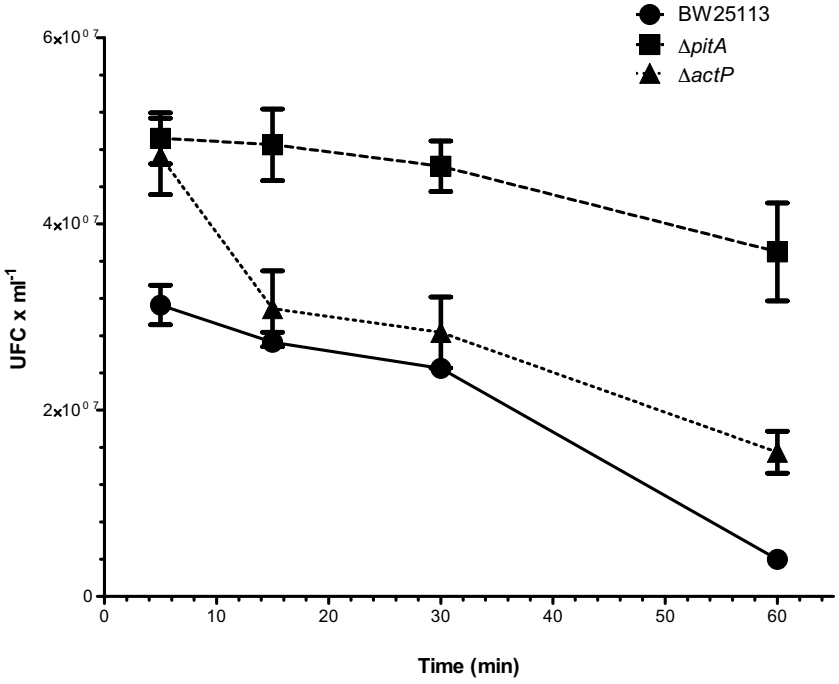


**Fig. 1.** Cell viability of *E. coli* BW25113 and mutant derivatives in the presence of tellurite. Cells were grown in M9 minimal medium supplemented with 0.2% glucose. The assay was performed as described in Section 2. Bars represent the average of 12 independent trials ± SE.

determined in the presence of cadmium, cobalt and zinc. While Δ*actP* cells exhibited higher resistance to $Cd^{2+}$ and $Zn^{2+}$ than the parental, isogenic strain, the Δ*pitA* strain showed increased zinc tolerance. Not one strain studied exhibited cobalt resistance (Table S2).

### 3.2. ROS generation assessment

Given that tellurite generates oxidative stress in the cell (Chasteen et al., 2009), it was interesting to determine if there was any correspondence among intracellular ROS and the different toxicant-exposed *E. coli* mutant strains. Time course experiments using $H_2$DCFDA showed that Δ*actP* cells exhibit lower levels of total ROS than any other strain, which remain almost constant with time (Fig. 2A). A similar trend was observed when superoxide was assessed. In spite of the fact that Δ*actP* cells showed a peak at 15 min, they still exhibited lower superoxide levels than the other strains under study (Fig. 2B).

### 3.3. Activity of antioxidant enzymes

Next, the cell response to toxicant exposure was analyzed more in depth. At short times after tellurite treatment (5 min) Δ*actP* cells showed ~50% less catalase activity than the other two strains analyzed (Fig. 3A). Under the same conditions, fumarase C activity in Δ*actP* was almost unchanged for the *E. coli* BW25113 control (Fig. 3B). A time course analysis (5–30 min) showed that catalase activity did not change in Δ*actP* cells while FumC activity increased

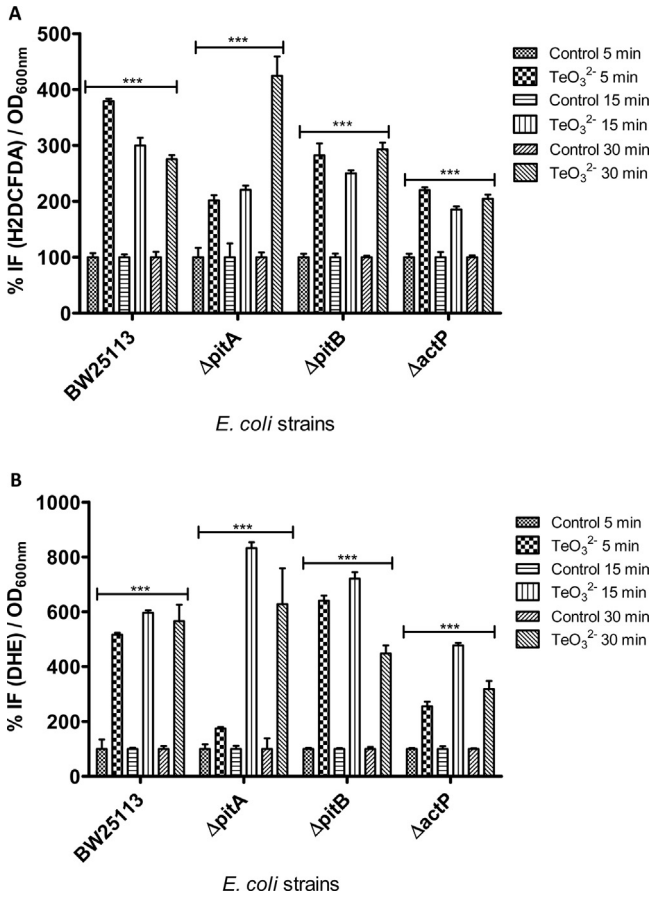


**Fig. 2.** Determination of reactive oxygen species. Total ROS (A) and superoxide content (B) measured in the indicated *E. coli* mutant strains in the presence of sub lethal tellurite concentrations. Bars represent the average of 3 independent trials ± SE; $p < 0.001$(***).

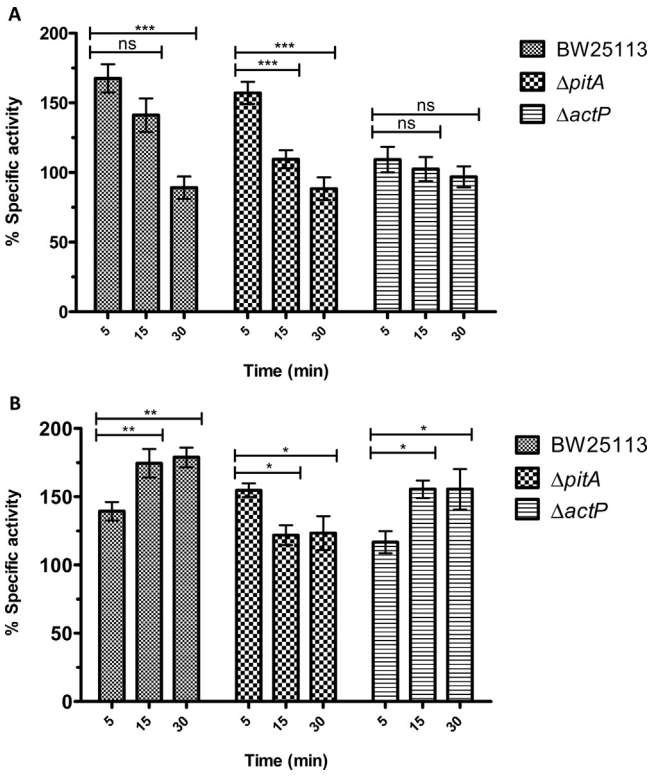


**Fig. 3.** Specific activity (%) of catalase (A) and FumC (B) in *E. coli* BW25113 and mutant derivatives at the indicated times of $TeO_3^{2-}$ exposure. Enzyme activity was determined as described in Section 2. Bars represent the average of 6 independent trials ± SE; $p < 0.05$(*), $p < 0.01$(**), $p < 0.001$(***); ns, not significant.

~50% at longer exposure times. The results shown in Figs. 2 and 3 strongly suggest that ActP is participating in tellurite uptake in *E. coli* (see below).

### 3.4. Kinetics of transport and intracellular tellurite content

While the toxicant concentration in supernatants of wild type cells dropped ~60% after 30 min exposure, the Δ*pitA* strain showed little change in extracellular tellurite content. In turn, residual tellurite in supernatants of *E. coli* Δ*actP* remained almost constant up to 5 min of exposure. Thereafter, tellurite entry increased showing a trend that was roughly in the middle of that exhibited by the parental BW25113 and Δ*pitA* strains (Fig. 4A).

The ability of ActP to deliver tellurite into *E. coli* was assessed using an *actP*-overexpressing strain (ASKA *actP*). After toxicant exposure, intracellular tellurite levels were determined by ICP-OES as described in Section 2. Clearly the ActP transporter is able to bring tellurite into *E. coli* (Fig. 4B), although to a lesser extent than PitA.

### 3.5. Relative gene expression in tellurite-exposed cells

The relative expression of tellurite transport-related genes (*pitA*, *pitB* and *actP*) and the antioxidant response genes *soxS* and *katG* were evaluated by qRT-PCR in time course experiments after exposing wild type *E. coli* to tellurite. Table 2 shows that while *actP* expression is slightly induced during the first 10 min, it is repressed at longer times. This is in agreement with the observation showing that *actP* operates mainly at short exposure times. In turn, *pitA* and *pitB* were subjected to an important induction at 15 min. As expected, *soxS* and *katG* (positive controls of oxidative stress-induced genes) were highly upregulated (Table 2).

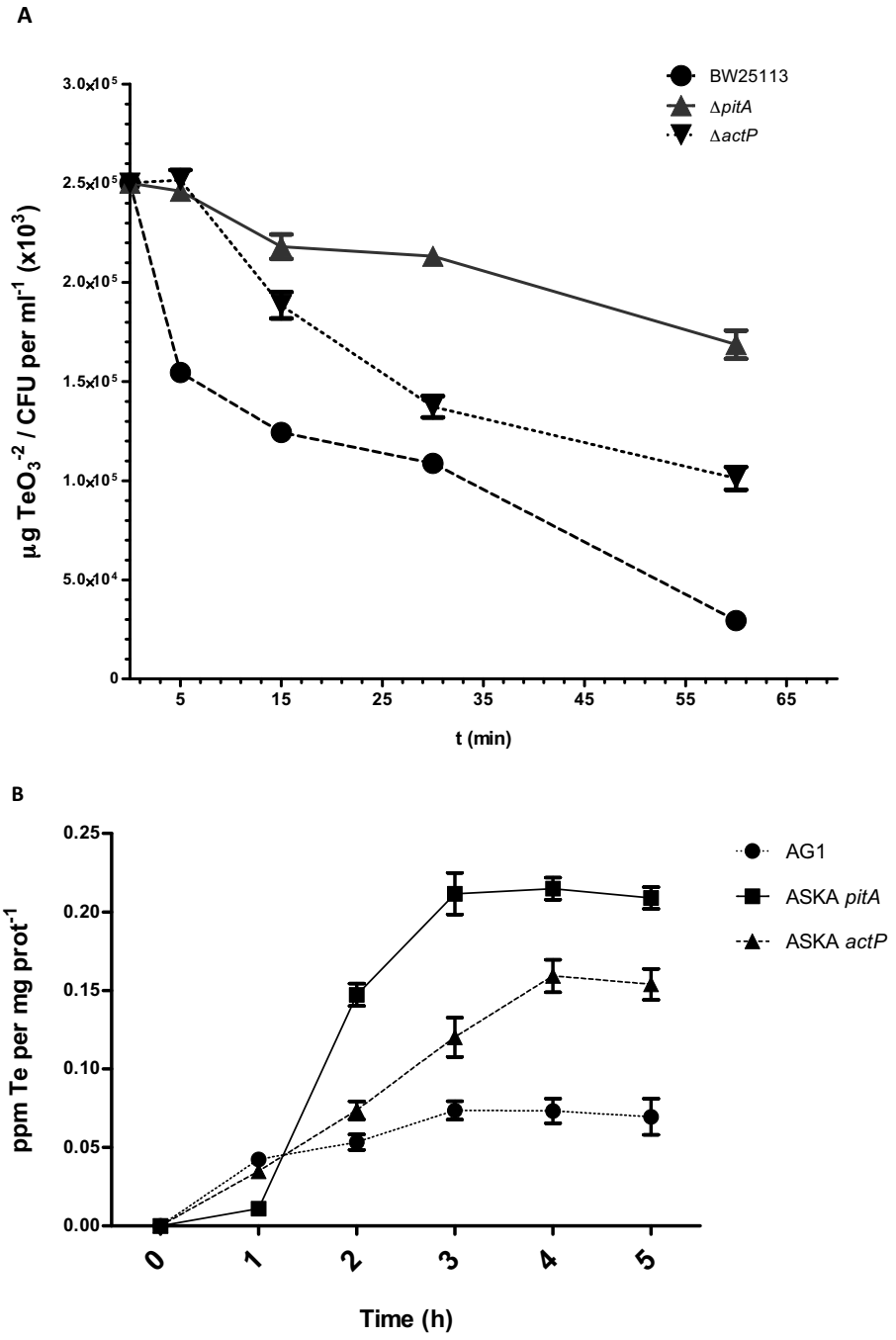


**Fig. 4.** Tellurium quantification. (A) Remaining extracellular tellurite in *Escherichia coli* cultures. Cells were grown to $OD_{600} \sim 0.15$ in M9-glucose medium, exposed to 20 μM $TeO_3^{2-}$; tellurite was determined in the supernatant at the indicated times. Results were normalized to the number of colony-forming units (CFU $ml^{-1}$). Bars represent the average of 9 independent trials ± SE. (B) Time course determination of intracellular tellurium species as determined by ICP-OES in cells previously exposed to tellurite. Bars represent the average of 3 independent trials ± SE.

Gene expression was also assessed in *E. coli* lacking *pitA*, *pitB*, *actP*, or *glpF*. An important induction of *actP* was observed in the Δ*pitB* strain. In turn, *pitA* and *pitB* induction was observed in *E. coli* Δ*actP* (Table 3).

## 4. Discussion

Bacterial tellurite toxicity is related to the generation of oxidative stress because of reduced thiol depletion and toxicant reduction that is accompanied by a concomitant superoxide production (Taylor, 1999; Chasteen et al., 2009; Lemire et al., 2013). Nevertheless, a key and less understood point is the way tellurite enters the cell. This transportation mechanism is important to unveil since tellurite is toxic only once it is in the intracellular compartment. Early in this investigation, Cooper and Few (1952) suggested that this process is very fast and stable at 25 °C and pH 5.5–7.0. Almost 35 years later, Tomás and Kay (1986) reported that tellurite entry was associated with phosphate transporters, an idea that found experimental support when Elías et al. (2012) demonstrated that the PitA phosphate transporter was the main protein or component responsible for tellurite entry to *E. coli*. In addition, Borghese et al. (2008) and Borghese and Zannoni (2010) showed that in *R. capsulatus* the process is pH-dependent and is associated with the ActP acetate transporter.

**Table 2**
Changes in relative gene expression in *E. coli* exposed to tellurite. Cells were grown in LB medium and exposed to tellurite (2 μM) for 5, 10 and 15 min, as indicated.

| Gene | Relative expression (fold) | | |
|---|---|---|---|
| | 5 min | 10 min | 15 min |
| *pitA* | 0.5 | 0.6 | 5.6 |
| *pitB* | 0.6 | 1.5 | 9.9 |
| *actp* | 1.4 | 1.2 | 0.3 |
| *soxS* | 4.3 | 108.6 | 12.3 |
| *katG* | 0.6 | 28.6 | 51.6 |

**Table 3**
Changes in relative gene expression in *E. coli* mutant strains. Cells were grown in LB medium and exposed to tellurite (2 μM) for 15 min; nd, not determined.

| Gene | Relative expression by mutant *E. coli* strain | | |
|---|---|---|---|
| | *ΔpitA* | *ΔpitB* | *Δactp* |
| *pitA* | nd | 114.6 | 4.3 |
| *pitB* | 1.8 | nd | 5.4 |
| *actP* | 0.6 | 20 | nd |
| *soxS* | 0.1 | 62.7 | 108.2 |
| *katG* | 0.4 | 2 | 2.5 |

These data prompted us to investigate more in depth myriad potential transporters that could be involved in tellurite entry to *E. coli*. A rapid screening of a number of mutant strains suggested that ActP could be involved in tellurite uptake (Table 1). The fact that Δ*glcA* and Δ*lacY* cells behave identically to the control *E. coli* BW25113 strain, indicated, most probably, that these transporters are not involved in tellurite entry and were, therefore, not investigated further.

On the other hand, growth curves and cell viability determinations indicated that ActP participation in tellurite entry to *E. coli* is less marked than that of the PitA phosphate transporter (Fig. 1 and Fig. S1). As expected, Δ*actP* cells exhibited lower levels of total ROS and superoxide than control cells, indicating a rather direct relationship between toxicant entry and intracellular ROS content (Fig. 2).

Given the above results, the activity of the antioxidant enzyme catalase was analyzed. At short times of tellurite exposure (5 min), catalase activity was lower in Δ*actP* than in parental cells, again indicating a lower oxidative harm (Fig. 3). As expected, upon longer exposure times, FumC activity – though with lower statistical significance – showed the same trend in Δ*actP* and the parental strain, a result that is in agreement with those observed for catalase activity. Taken together, these findings allow us to infer that Δ*actP* cells are less stressed by exposure to tellurite. More important, FumC activity remained relatively constant at times >5 min in Δ*pitA*. Since these cells contain a functional *actP* gene, one would expect that tellurite entered the cells only up to 5 min or less thus explaining the drop of FumC activity at 10 and 15 min treatment.

To corroborate the assumption that ActP is able to carry tellurite, a kinetic analysis of toxicant uptake was conducted (Fig. 4A). Given that at short exposure time (5 min) the extracellular toxicant concentration remains constant and drops almost exponentially thereafter, we conclude that ActP would mediate early tellurite entry into *E. coli*, a mission that is switched to the PitAB system at longer toxicant treatments. ICP-OES experiments confirmed that both ActP as well as PitAB can help tellurite entry to *E. coli* (Fig. 4B). This could be considered indirect evidence of an important toxicant versatility to mimic the entry of other molecules of biological importance, which in turn could explain the high tellurite toxicity for most microorganisms.

Summarizing, the results strongly suggest that, at least in *E. coli*, tellurite uptake is a multifactor event that involves at least two transporters: ActP, very active at short times of exposure, and the PitAB system, more relevant at longer exposures to the toxicant. This phenomenon could be explained taking into consideration the anaerobic switch that results when this bacterium faces the toxicant (Molina-Quiroz et al., 2014). Since *actP* is under regulation by the *acs* operon – which operates chiefly under aerobic conditions (Kumari et al., 1995) – toxicant treatment would have a very fast effect in *actP* expression and thus in its participation in tellurite uptake (Tables 2 and 3). Another interesting interpretation is related to the transporter's particular action mechanism. While ActP is a symporter associated with the $Na^+$ gradient, the PitAB system is dependent on the transmembrane proton gradient (Harris et al., 2001). Along this line, it has been recently shown that tellurite affects the *E. coli* electron transport chain (Díaz-Vásquez et al., 2014b) and hence ATP generation (Lohmeier-Vogel et al., 2004). This would have two important effects on ActP: alteration of the transmembrane $Na^+$ gradient and the inhibition of the *acs* operon, which would cause a decrease in *actP* expression.

Finally, other toxic metal ions generating intracellular damage were tested through the determination of growth inhibition zones. The results showed that the Δ*actP* mutant exhibited resistance to $Zn^{2+}$ and $Cd^{2+}$ but not to $Co^{2+}$ (Table S2). Further studies to unveil more in depth the participation of these and other transporters in tellurite entry to *E. coli* and/or the effects of other toxicants in this process are being carried out in our laboratory.

## Acknowledgements

This work was supported in part by grant nos. 1090097 and 1130362 from Fondecyt and Dicyt-USACH, to C.C.V. F.A.S was supported by Fondecyt Initiation Into Research grant no. 11140334. T.G.C. was supported by grant no. X-011 from the Robert A. Welch Foundation.

## Appendix A. Supplementary data

Supplementary data associated with this article can be found, in the online version, at http://dx.doi.org/10.1016/j.micres.2015.04.010

## References

Acuña L, Calderón I, Elías A, Castro M, Vásquez C. Expression of the *yggE* gene protects *Escherichia coli* from potassium tellurite-generated oxidative stress. Arch Microbiol 2009;191(5):473–6.

Araya MA, Swearingen JW Jr, Plishker MF, Saavedra CP, Chasteen TG, Vásquez CC. *Geobacillus stearothermophilus* V *ubiE* gene product is involved in the evolution of dimethyl telluride in *Escherichia coli* K-12 cultures amended with potassium tellurate but not with potassium tellurite. J Biol Inorg Chem 2004;9(5):609–15.

Baba T, Ara T, Hasegawa M, Takai Y, Okumura Y, Baba M, et al. Construction of *Escherichia coli* K-12 in-frame, single-gene knockout mutants: the Keio collection. Mol Syst Biol 2006;2, 2006.0008.

Borghese R, Marchetti D, Zannoni D. The highly toxic oxyanion tellurite ($TeO_3^{2-}$) enters the phototrophic bacterium *Rhodobacter capsulatus* via an as yet uncharacterized monocarboxylate transport system. Arch Microbiol 2008;189(2):93–100.

Borghese R, Zannoni D. Acetate permease (ActP) is responsible for tellurite ($TeO_3^{2-}$) uptake and resistance in cells of the facultative phototroph *Rhodobacter capsulatus*. Appl Environ Microbiol 2010;76(3):942–4.

Borsetti F, Toninello A, Zannoni D. Tellurite uptake by cells of the facultative phototroph *Rhodobacter capsulatus* is a ΔpH-dependent process. FEBS Lett 2003;554(3):315–8.

Borsetti F, Tremaroli V, Michelacci F, Borghese R, Winterstein C, Daldal F, et al. Tellurite effects on *Rhodobacter capsulatus* cell viability and superoxide dismutase activity under oxidative stress conditions. Res Microbiol 2005;156(7):807–13.

Bradford MM. A rapid and sensitive method for quantification of microgram quantities of protein utilizing the principles of protein-dye binding. Anal Biochem 1976;72(1–2):248–54.

Calderón IL, Elías AO, Fuentes EL, Pradenas GA, Castro ME, Arenas FA, et al. Tellurite-mediated disabling of [4Fe–4S] clusters of *Escherichia coli* dehydratases. Microbiology 2009;155(6):1840–6.

Castro ME, Molina R, Díaz W, Pichuantes SE, Vásquez CC. The dihydrolipoamide dehydrogenase of *Aeromonas caviae* ST exhibits NADH-dependent tellurite reductase activity. Biochem Biophys Res Commun 2008;375(1):91–4.

Castro ME, Molina RC, Díaz WA, Pradenas GA, Vásquez CC. Expression of *Aeromonas caviae* ST pyruvate dehydrogenase complex components mediate tellurite resistance in *Escherichia coli*. Biochem Biophys Res Commun 2009;380(1):148–52.
Chasteen TG, Fuentes DE, Tantaleán JC, Vásquez CC. Tellurite: history, oxidative stress, and molecular mechanisms of resistance. FEMS Microbiol Rev 2009;33(4):820–32.
Chasteen TG, Bentley R. Biomethylation of selenium and tellurium: microorganisms and plants. Chem Rev 2003;103(1):1–25.
Chen G, Schellhorn HE. Controlled induction of the RpoS regulon in *Escherichia coli*, using an RpoS-expressing plasmid. Can J Microbiol 2003;49(12):733–40.
Chiong M, González E, Barra R, Vásquez C. Purification and biochemical characterization of tellurite-reducing activities from *Thermus thermophilus* HB8. J Bacteriol 1988;170(7):3269–73.
Cooper PD, Few AV. Uptake of potassium tellurite by a sensitive strain of *Escherichia coli*. Biochem J 1952;51(4):552–7.
Cunha RL, Gouvea IE, Juliano L. A glimpse on biological activities of tellurium compounds. An Acad Bras Cienc 2009;81(3):393–407.
Díaz-Vásquez WA, Abarca-Lagunas MJ, Arenas FA, Pinto CA, Cornejo FA, Wansapura PT, et al. Tellurite reduction by *Escherichia coli* NDH-II dehydrogenase results in superoxide production in membranes of toxicant-exposed cells. Biometals 2014a;27(2):237–46.
Díaz-Vásquez WA, Abarca-Lagunas MJ, Cornejo FA, Pinto CA, Arenas FA, Vásquez CC. Tellurite-mediated damage to the *Escherichia coli* NDH-dehydrogenases and terminal oxidases in aerobic conditions. Arch Biochem Biophys 2014b;15(566):67–75.
Elías AO, Abarca MJ, Montes RA, Chasteen TG, Pérez-Donoso JM, Vásquez CC. Tellurite enters *Escherichia coli* mainly through the PitA phosphate transporter. MicrobiologyOpen 2012;1(3):259–67.
Fleming A. On the specific antibacterial properties of penicillin and potassium tellurite. J Pathol Bacteriol 1932;35(6):831–42.
Fuentes DE, Fuentes EL, Castro ME, Pérez JM, Araya MA, Chasteen TG, et al. Cysteine metabolism-related genes and bacterial resistance to potassium tellurite. J Bacteriol 2007;189(24):8953–60.
Harris RM, Webb DC, Howitt SM, Cox GB. Characterization of PitA and PitB from *Escherichia coli*. J Bacteriol 2001;183(17):5008–14.
Kitagawa M, Ara T, Arifuzzaman M, Ioka-Nakamichi T, Inamoto E, Toyonaga H, et al. Complete set of ORF clones of *Escherichia coli* ASKA library (a complete set of *E. coli* K-12 ORF archive): unique resources for biological research. DNA Res 2005;12(5):291–9.
Kumari S, Tishel R, Eisenbach M, Wolfe AJ. Cloning, characterization, and functional expression of *acs*, the gene which encodes acetyl coenzyme A synthetase in *Escherichia coli*. J Bacteriol 1995;177(10):2878–86.
Lemire JA, Harrison JJ, Turner RJ. Antimicrobial activity of metals: mechanisms, molecular targets and applications. Nat Rev Microbiol 2013;11(6):371–84.
Liochev SI, Fridovich I. Fumarase C, the stable fumarase of *Escherichia coli*, is controlled by the *soxRS* regulon. Proc Natl Acad Sci USA 1992;89(13):5892–6.
Livak KJ, Schmittgen TD. Analysis of relative gene expression data using real-time quantitative PCR and the 2(−Delta Delta *C*(*T*)). Methods 2001;25(4):402–8.
Lohmeier-Vogel EM, Ung S, Turner RJ. In vivo $^{31}$P nuclear magnetic resonance investigation of tellurite toxicity in *Escherichia coli*. Appl Environ Microbiol 2004;70(12):7342–7.
Meng YL, Liu Z, Rosen BP. As(III) and Sb(III) uptake by GlpF and efflux by ArsB in *Escherichia coli*. J Biol Chem 2004;279(18):18334–41.
Molina RC, Burra R, Pérez JM, Elías AO, Muñoz C, Montes RA, et al. Simple, fast, and sensitive method for quantification of tellurite in culture media. Appl Environ Microbiol 2010;76(14):4901–4.
Molina-Quiroz RC, Loyola DE, Díaz-Vásquez WA, Arenas FA, Urzúa U, Pérez-Donoso JM, et al. Global transcriptomic analysis uncovers a switch to anaerobic metabolism in tellurite-exposed *Escherichia coli*. Res Microbiol 2014;165(7):566–70.
Moscoso H, Saavedra C, Loyola C, Pichuantes S, Vásquez C. Biochemical characterization of tellurite-reducing activities of *Bacillus stearothermophilus* V. Res Microbiol 1998;149(6):389–97.
Nies DH. Microbial heavy-metal resistance. Appl Microbiol Biotechnol 1999;51(6):730–50.
Pérez JM, Calderón IL, Arenas FA, Fuentes DE, Pradenas GA, Fuentes E, et al. Bacterial toxicity of potassium tellurite: unveiling an ancient enigma. PLoS ONE 2007;2(2):e211.
Pradenas GA, Díaz-Vásquez WA, Pérez-Donoso JM, Vásquez CC. Monounsaturated fatty acids are substrates for aldehyde generation in tellurite-exposed *Escherichia coli*. Biomed Res Int 2013;2013:563756.
Sambrook J, Russell DW. Molecular cloning: a laboratory manual. 3rd ed. NY: Cold Spring Harbor Laboratory Press; 2001.
Sanders OI, Rensing C, Kuroda M, Mitra B, Rosen BP. Antimonite is accumulated by the glycerol facilitator GlpF in *Escherichia coli*. J Bacteriol 1997;179(10):3365–7.
Taylor DE. Bacterial tellurite resistance. Trends Microbiol 1999;7(3):111–5.
Tomás JM, Kay WW. Tellurite susceptibility and non-plasmid-mediated resistance in *Escherichia coli*. Antimicrob Agents Chemother 1986;30(1):127–31.
Turner RJ, Weiner JH, Taylor DE. Tellurite-mediated thiol oxidation in *Escherichia coli*. Microbiology 1999;145(9):2549–57.
Turner MS, Tan YP, Giffard PM. Inactivation of an iron transporter in *Lactococcus lactis* results in resistance to tellurite and oxidative stress. Appl Environ Microbiol 2007;73(19):6144–9.
Valdivia-González M, Pérez-Donoso JM, Vásquez CC. Effect of tellurite-mediated oxidative stress on the *Escherichia coli* glycolytic pathway. Biometals 2012;25(2):451–8.